

# Impact of Short Chain Branching on Conformations of Metallocene LLDPE Melts: NMR, Light Scattering and MD Simulation Study

Nasiru M. Tukur,<sup>\*1</sup> Basel F. Abu Sharkh,<sup>1</sup> Emmanuel Y. Osei-Twum,<sup>2</sup> Ibbelwaleed A. Hussein<sup>1</sup>

**Summary:** The influence of short chain branching on molecular conformations of melts and solutions of metallocene linear Low-density polyethylene (*m*-LLDPE) was studied by nuclear magnetic resonance (NMR) spectroscopy, light scattering, and Molecular Dynamics (MD) simulation techniques. Both  $T_2$  relaxation measurements by NMR and MD simulations suggest the loss of molecular order in *m*-LLDPE at temperatures  $>135^\circ\text{C}$ . Similar trends were observed for the radius of gyration as measured by light scattering and calculated from MD simulations vs. branch content (BC) and type. At high BC ( $>40$  branches/1000 C) *m*-LLDPE tends towards self assembly. Neither the branch type nor the BC has significant effect on the intermolecular orientation correlation function. This might be attributed to the fact that the high temperature of the melt results in loss of order in the chains. This lack of order is independent of BC or type. This result is in agreement with the results of the dihedral distribution analysis. Also, it is in agreement with our NMR  $T_2$  measurements. The radial distribution functions are nearly identical indicating no effect of branch type at low branch density on the correlation between branches and backbone segments. However, increasing the BC to 80 branches/1000C resulted in a change in the correlation between the branches and backbone segments.

**Keywords:** light scattering; linear low density polyethylene; *m*-LLDPE; molecular dynamics; NMR; Short chain branching

## Introduction

Polyethylene (PE) occupies an important position in the commodity plastics market. The demand for PE as a raw material for synthetic polyester continues to grow and drive the search to increase PE production processes. It is estimated that the nearly

100 million metric tons of synthetic polymers are produced per year worldwide.

The development of polyethylene production technology did not proceed smoothly. It demanded untiring efforts before the utility of synthetic polymers was appreciated. The chance discovery in 1935 that ethene can be polymerized at very high pressure to produce a high molecular weight semi-crystalline material was the starting point of the manufacture of polyethylene.

Initially, polyethylene was a highly branched low density material with a limited range of physical properties. In the 1950s, new catalytic polymerization processes were developed that produced essentially

<sup>1</sup> Department of Chemical Engineering, King Fahd University of Petroleum & Minerals, Dhahran 31261, Saudi Arabia  
Tel.: +966-3-860-2757; Fax: +966-3- 860-4234  
E-mail: nmtukur@kfupm.edu.sa

<sup>2</sup> Research Institute, King Fahd University of Petroleum & Minerals, Dhahran 31261, Saudi Arabia

linear polymers with higher densities. In the 1960s, the copolymerization of ethylene with small amounts of other  $\alpha$ -olefins produced linear low density polyethylene (LLDPE). Metallocene catalysts have been known for several decades. However, their potential as commercial catalysts remained unrealized until 1980, when Kaminsky and coworkers<sup>[1]</sup> discovered that the methylalumoxane co-catalyst improved their catalytic activity dramatically. Since that discovery, massive and intense research programs have been undertaken to bring metallocene products to commercial use. The most remarkable feature of these catalyst systems is the fact that all metallocene sites produce polymer chains with virtually the same architecture. The catalyst also produces polymers with narrow molecular weight distribution, higher comonomer contents, and good compositional homogeneity. Metallocene catalyzed elastomeric very low density polyethylene (VLDPE) resins became available commercially in 1993. The metallocene LLDPE (*m*-LLDPE) products followed in 1995 as reported by Peacock.<sup>[2]</sup>

Ziegler-Natta LLDPE resins consist of molecules with linear polyethylene (LPE) backbones to which are attached short alkyl groups at random intervals. These materials are produced by the copolymerization of ethylene with 1-alkene comonomers. These comonomers are typically  $\alpha$ -olefins, principally 1-butene, 1-hexene, and 1-octene. LLDPE resins may also contain small levels of long chain branching as is found in low density polyethylene (LDPE). Chemically, these resins can be thought of as a compromise between LPE and LDPE, hence the name LLDPE.<sup>[2]</sup>

There are two types of LLDPE available in the market, conventional Ziegler-Natta (ZN-LLDPE) and *m*-LLDPE. Metallocene-type ethylene- $\alpha$ -olefin copolymers are characterized by their narrow molecular weight distribution ( $2.0 \leq \text{polydispersity index} \leq 3.5$ ) and almost homogeneous comonomer composition distribution. This is in contrast to Ziegler-Natta copolymers, which are broadly poly-dispersed in terms of mole-

cular weight and composition. Here, the longer molecules incorporate a lower percentage of comonomers than the shorter ones as indicated by Stevens.<sup>[3]</sup>

Numerous MD simulation studies by several groups have been conducted on polyethylene.<sup>[4,5]</sup> However, most of the PE simulation studies were mainly on LPE chains. One of the few studies that addressed branched PE is that of Choi,<sup>[6]</sup> which examined the miscibility of branched polyethylene blends using MD simulation. Recent studies by Zhang et al.<sup>[7]</sup> reported the role of uniformly distributed branching resulting from copolymerization of ethylene with butene and propene on crystal structure of branched polyethylene. Abu-Sharkh and Hussein<sup>[8]</sup> studied the influence of branch content (BC) on conformation of Ziegler-Natta linear-low density polyethylene (ZN-LLDPE) in dilute solutions using molecular dynamics simulation. Octene LLDPE with different levels of BC distributed *randomly* along the chain mimicking ZN-LLDPE were simulated in vacuum at 400 and 500 K. Increasing BC was found to decrease chain folding and with an effect on the chain conformation. They determined that chain conformation undergoes transition from lamellar to a more random coil-like structure near a BC of 40 branches/1000 backbone carbons. A similar systematic investigations of the influence of random branching on chain folding, conformation and order in PE chains in the melt have not been reported.

The present study is aimed at investigating the influence of short chain branching on conformations of melts and solutions of metallocene linear Low-density polyethylene (*m*-LLDPE) using nuclear magnetic resonance (NMR) spectroscopy, light scattering, and Molecular Dynamics (MD) simulation techniques. Dihedral distribution functions, orientation correlation functions and intermolecular radial distribution functions will be determined and analyzed for a number of selected short branch contents and type in order to determine their influences on the molecular order of the melt structure.

## Molecular Dynamics (MD) Simulation

### Methodology

For the purpose of molecular simulation, PE chain models composed of 100 repeating units (200 backbone carbons) are constructed. End methyl ( $\text{CH}_3$ ) groups and backbone methylene ( $\text{CH}_2$ ) groups are modeled using united atom representation (UA). ZN-LLDPE chains with branches ranging in size from two carbons (butene) to 6 carbons (octene) and in branch density ranging from 20 to 80 branches/1000 C are used. The branches in these chains are evenly distributed to mimic metallocene LLDPEs. Simulations are started by constructing an amorphous cell containing the chains with densities that are similar to the experimental densities of the melts. The MD simulations are carried out in the NVT ensemble.

Dispersion interactions between non-bonded atoms are described using a Lennard-Jones (L-J) 6–12 potential energy function of the form:

$$U^{LJ}(r_{ij}) = \varepsilon[(r_{ij}^0/r_{ij})^{12} - 2(r_{ij}^0/r_{ij})^6] \quad (2.1)$$

where  $r_{ij}$  is the separation between atoms  $i$  and  $j$ . The non-bonded interactions were applied to groups separated by more than two bonds. Non-bonded dispersion interactions were truncated using a cutoff radius of 10 Å with continuum corrections in order to limit the number of interactions without affecting properties of the system seriously.

The force field used to model the chains is the PCFF force field and is described by an equation of the form (Sun et al.,<sup>[9,10]</sup>). The force field employs a quartic polynomial for bond stretching, angle bending, a three-term Fourier expansion for torsions, Coulombic interaction between the atomic charges and van der Waals interactions. Nonbonded van der Waals interactions were calculated with a cutoff distance of  $2.5\sigma$ , where  $\sigma$  is diameter of a chain bead. Standard long range corrections were applied. Simulations are carried out in the NVT ensemble with periodic boundary

conditions. A constant temperature was accomplished by linking the system to a thermostat. A simulation time step of 3 fs was used. The initial extended chains were allowed to equilibrate in the NVT ensemble as conformation of the chain is observed with time.

### Simulation of the Melt

Chains of Linear low density PE composed of 100  $\text{CH}_2$  units each with various types of branches and branch densities are constructed using united atom representation where  $\text{CH}_2$  and  $\text{CH}_3$  segments are represented by a single bead. 10 chains were initially placed in a periodic cubic simulation box using the *Materials Studio* amorphous builder. The box was then equilibrated in a low-density periodic box at 600 K. After simulation for 0.5 ns at the elevated temperature of 600 K, the temperature was reduced to 500 K. The system was simulated for 1 ns at constant pressure. The pressure was increased until the density of the system was equivalent to the experimental density of the system under investigation at 500 K. The pressure was then fixed and the pressure and energy were monitored for 8–10 ns to ensure equilibration. The system was then simulated in the canonical (NVT) ensemble using the Nose-Hoover method.<sup>[10]</sup>

The simulations were carried out using the discover module of Materials Studio molecular modeling code (Accelrys Inc.). Periodic boundary conditions were applied and the systems were simulated in the melt with the temperature kept constant at 500 K. Melting was ensured by measuring the density of the system as a function of temperature in the range from 300 K to 600 K. Melting is indicated by a change in the slope of the specific volume with temperature. An integration time step of 0.003 ps was used. A relaxation constant of 0.1 for the relaxation heat variable bath was applied throughout the simulations.

To study the effect of branch density and type on melt structure, we followed the procedure outlined in a previous publication.<sup>[8]</sup> The dihedral distribution functions,

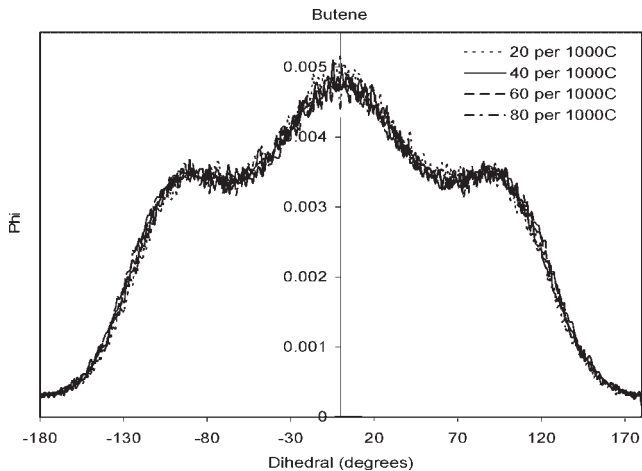


**Figure 1.**  
Dihedral angle analysis (BT: Butene).

orientation correlation functions and intermolecular radial distribution functions are analyzed for all systems.

### MD Simulation – Results and Discussion

#### Dihedral Distribution

The dihedral angle distribution was determined for the equilibrated melt of polymers with octene, hexene and butene branches and containing 20, 40, and 80 branches per

1000 C. Figure 1 shows the influence of branch content on dihedral distribution for the same branch type.

The figure shows that branch type has very little influence on the dihedral angle distribution of the backbone. In general, the dihedral distribution in branched PE melts is not strongly influenced by branch content up to 80 branches/1000 C and is very little influenced by branch type, with the 20 branches per 1000C having the

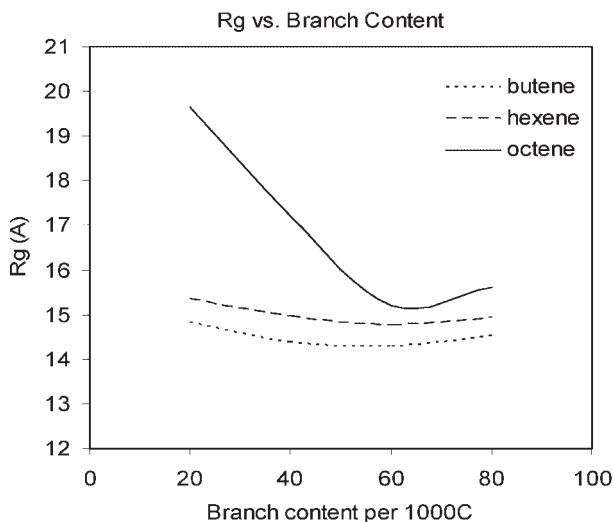


**Figure 2.**  
Radius of gyration against branch content.

highest trans population. This is caused by the increased steric hindrance caused by the larger branches for the backbone to assume the trans configuration.

#### Radius of Gyration

The radius of gyration of polymers with different branch content and branch types was analyzed. Figure 2 displays results of the analysis. It can be observed that the octene branched polymer has the largest  $R_g$  followed by the hexane then the butane branched polymers. This can be attributed to the inability of the chains with large branches to fold into compact coils. As a result, the chain has an expanded coil structure with large radius and lower mass density. This result is in agreement with experimental observations that PE with longer branches has lower density.

#### Intermolecular Orientation Correlation

Figure 3 shows the intermolecular orientation correlation function for the PE with different branch content and type. The figure shows that neither the branch type nor the branch content has significant effect on the intermolecular orientation correlation function. This might be attributed to

the fact that the high temperature of the melt results in loss of order in the chains. This lack of order is independent of branch content or type. This result is in agreement with the results of the dihedral distribution analysis. It is clear that the high temperature of the melt results in overcoming the energy barriers to rotation, hence the loss of order that is observed. However, all systems are characterized by a certain level of intermolecular order that extends for up to 10 Å.

#### Radial Distribution Function (rdf)

ZN-LLDPEs are characterized by heterogeneous distribution of branches along the backbone. Figure 4 shows the correlation function between parts of the chain that contain branches with linear un-branched parts.

For the butene branched polymer, the correlation is maximum for the polymers with low branch density. The correlation generally decreases with increasing branch content and is at minimum for chains with 80 branches per 1000C. This indicates that branches result in structural heterogeneity within the melt with branched parts of the molecules assembling away from the linear parts. The same phenomenon applies for the hexane and octene branches. However,

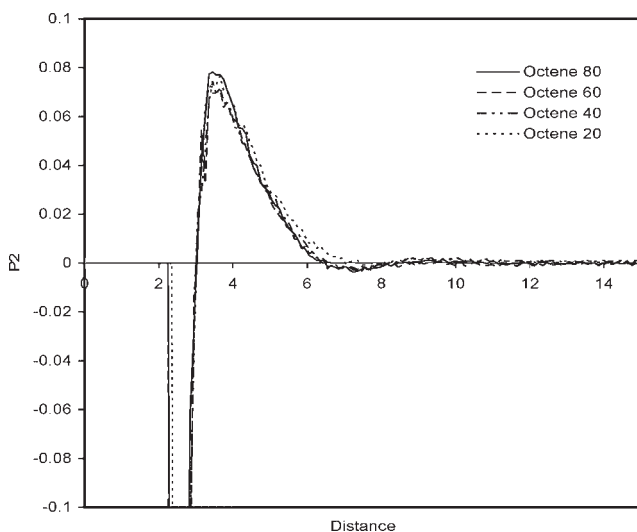


**Figure 3.** Intermolecular orientation correlation function for the PE with different branch.

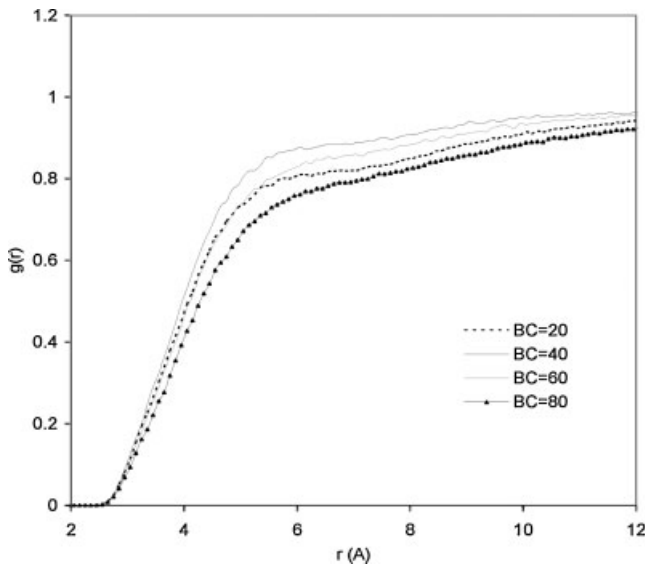


**Figure 4.**

Backbone branched-backbone linear rdf comparison (PE-ZN-Butene).

polymers with shorter branches are influenced to a larger extent by branch density. This indicates that shorter branches influence the correlation between linear and branched segments of the chains only at high branch density.

## Light Scattering

### Methodology

Laser light scattering is the only method available for determination of the absolute molecular weight of polymers. It can be used to determine the number, weight and Z-average molecular mass of polymers. It can be also used to determine molecular sizes by measuring the variation of scattering with angle. Furthermore, information about the level of branching in a molecule and aggregation between molecules can be easily obtained. The laser light instrument works by exposing a sample to a polarized laser beam. The sample scatters light in all directions. Detectors placed at different angular positions around the sample provide a response proportional to the inten-

sity of light scattered in its direction (Waters 2000 GPC equipment was utilized). The scattered light data is analyzed by solving the following equation:

$$\frac{Kc}{R(\theta)} = \frac{1}{M_w P(\theta)} + 2A_2 c \quad (3.1)$$

$R(\theta)$  is the excess Rayleigh ratio,  $c$  is the molecular concentration,  $M_w$  is the weight average molecular mass,  $A_2$  is the second virial coefficient,  $K$  is a function of the refractive index of the solvent, molecule and concentration of the polymer and  $P(\theta)$  is the form factor which depends on the structure of the scattering molecule from which the mean square radius may be determined. The quantities on the left hand side are measurable quantities. Analytical software finds the best values of the three unknowns on the right hand side, which are  $M_w$ ,  $A_2$  and the mean square radius. As we can see, the results are obtained from fundamental measurements and no empirical formulae or molecular weight standards are needed.

Light scattering was used to determine the influence of short chain branching on

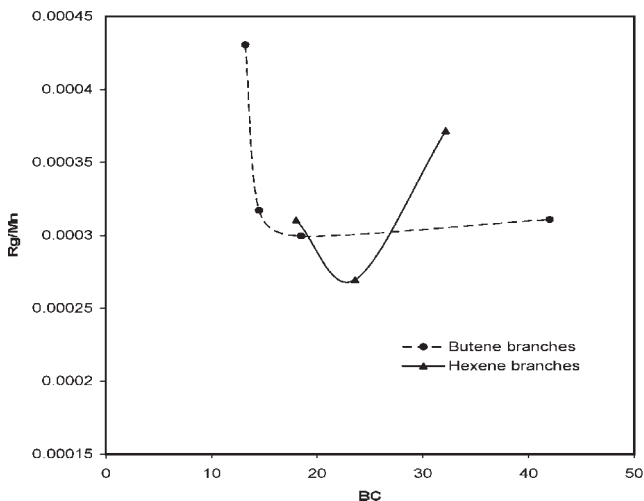


**Figure 5.**

A plot of  $R_g/M_n$  Vs Branch content (based on experimental  $R_g$ ).

the size and shape of the PE chains. First, it was used to characterize the molecular weight of the polymers in solution, and then radius of gyration ( $R_g$ ) of the chains correlated with the  $M_w$  using a power law relationship of the form:

$$R_g = KM_w^a \quad (3.2)$$

The exponent  $a$  is related to the branch content.

### Light Scattering – Results and Discussion

The radius of gyration of polymers with different branch content and branch types determined using the light scattering technique are presented in Figure 5. The  $R_g$  was normalized by molecular weight in order to be able to isolate the effect of branch content and type on  $R_g$ . It can be observed from Figure 5 that there is sharp drop in the  $R_g/M_n$  value as the branch content increases and then a slow or sharp increase depending on the type of branch. A similar trend was observed in Figure 2, where  $R_g$  from simulation was plotted against branch content. However, the value of the critical branch content where the chain collapse takes place is different in the two plots. This may be attributed to errors in the experimentally determined  $R_g$ .

## Nuclear Magnetic Resonance (NMR)

### Methodology

Over the years, nuclear magnetic resonance spectroscopy commonly referred to as NMR, has become the best technique for determining the structure of organic compounds.  $T_2$  relaxations of samples of *m*-LLDPE were carried out using NMR to identify temperature effect on the spin-spin relaxation.

The  $T_2$  measurements were done on a JEOL JNM-GX270 spectrometer at a frequency of 270 MHz operating in the quadrature detection mode. Several probe sequences have been developed for the  $T_2$  measurements, the most popular being the Carr-Purcell technique. This sequence has been modified by Meiboom and Gill. The Carr-Purcell-Meiboom-Gill technique was used with the pulse train being:

$$90_x - (D_2 - 180_{xy} - D_2)_c - DE - AQ \quad (4.1)$$

In this train there is an initial  $90^\circ$  pulse, phase-controlled, followed by a fixed delay time,  $D_2$ . This delay time, which is to allow for dephasing of the magnetization in the

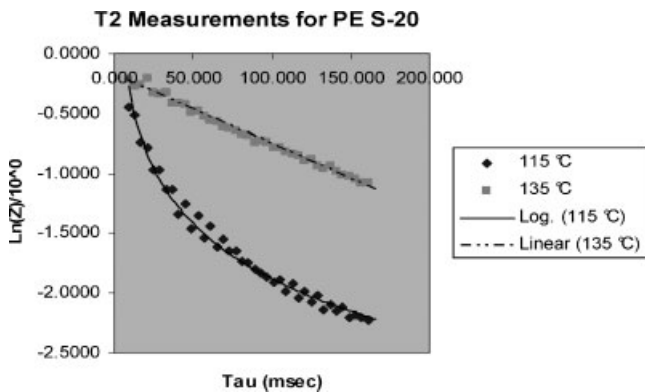


Figure 6.

$T_2$  relaxation plot of molten LLDPE S-20 at 115 °C and 135 °C.

XY plane, will be set at about 0.6 ms. After this time, a 180° pulse is applied, phase shifted 90° from the initial 90° pulse, so that the magnetization is rotated upon the central Y' axis in the 3-D frame of reference. This 180° refocusing pulse allows the isochromats to refocus towards the Y' axis during the second  $D_2$  delay. After the second short delay, the resulting magnetization is detected and the free induction decay is obtained. The subscript c in the pulse train is a variable, which is used to control the number of times that the  $D_2 - 180_{xy} - D_2$  sequence is run through before the actual acquisition. The presence of paramagnetic impurities such as molecular oxygen in a sample is known to affect the relaxation mechanism strongly by providing a highly efficient dipolar relaxation pathway. For this reason the sample was extensively degassed for 40 hours or more under vacuum better than  $10^{-6}$  torr and then the tube sealed.

### NMR – Results and Discussion

The  $T_2$  relaxations of a total of 20 metallocene linear low density polyethylene (LLDPE) samples were measured. Two types of polyethylenes were identified. The first type have a linear plot of  $\text{Ln}(z)$  vs.  $\tau$  (tau) where  $z$  is  $A/A_0$  ( $A$  is the echo amplitude). Figure 6 shows representations of these plots.

As a result of the wide molecular weight distribution of the commercial-grade polyethylene, one should expect that the molten polymer would contain entangled and unentangled constituents. The analysis of the NMR absorption spectra and spin-spin ( $T_2$ ) relaxation decays of polyethylene melts by Zachmann and Gölz<sup>[11]</sup> showed the existence of two to four discrete components. Bremner and Rudin<sup>[12]</sup> have confirmed the existence of such entangled structures in the solid and molten polyethylene.

The spin-spin relaxation in polymer melts decays gradually changes from the exponential time dependency to a linear one. This indicates that the characteristics of molten polymers changes as the temperature is raised. This is illustrated by PE S-20 in Figure 6. The Figure also shows that at the lower temperature, the polymer melt contains both the entangled and unentangled components while at the higher temperature, the entangled component becomes unentangled and the whole polymer becomes homogeneous. It appears that some of the PEs that showed a linear relationship at 135 °C exhibited the features of entanglement at lower temperatures or in the pure solid. This suggests that molecular order in PEs is lost at temperatures much higher than the 135 °C at atmospheric pressure. These results are in agreement with our conclusions from intermolecular orientation correlation function.

## Conclusions

The following conclusions can be drawn from the investigation of the influence of short chain branching on molecular order of melts and solutions of metallocene linear Low-density polyethylene (*m*-LLDPE) using nuclear magnetic resonance (NMR) spectroscopy, light scattering, and Molecular Dynamics (MD) simulation techniques.

- In general, the dihedral distribution in branched PE melts is not strongly influenced by branch content up to 80 branches/1000 C and is very little influenced by branch type with the 20 branches per 1000C having the highest trans population.
- Neither the branch type nor the BC has significant effect on the intermolecular orientation correlation function. This might be caused by the fact that the high temperature of the melt results in loss of order in the chains. This lack of order is independent of BC or type. This result is in agreement with the results of the dihedral distribution analysis. Also, it is in agreement with our NMR T2 measurements.
- At high BC, branches tend more towards self assembly. It was observed that longer branches showed less correlation with backbone segments and tend to self assemble.
- The characteristics of the molten polymers changed as the temperature was raised. The spin-spin relaxation decays gradually changed from the exponential

time dependency to a linear one. This suggests that molecular order in PEs is lost at temperatures much higher than the 135°C at atmospheric pressure. These results are in agreement with our conclusions from intermolecular orientation correlation function.

*Acknowledgements:* This project is supported by the King AbdulAziz City for Science and Technology (KACST) under project # AT-22-16. Also, the support of King Fahd University of Petroleum and Minerals is highly appreciated.

- [1] W. Kaminsky, M. Miri, H. Sinn, R. Woldt, *Macromolecular Chemistry Rapid Communication*, **1983**, 4, 417.
- [2] J. Peacock, in "Handbook of Polyethylene: Structures, Properties, and Applications", 1<sup>st</sup> ed., Marcel Dekker, **2000**.
- [3] J. C. Stevens, J.C., *Studies in Surface Science & Catalysis*, **1996**, 101, 11.
- [4] D. Rigby, R. J. Roe, in "Computer Simulation of Polymers", Prentice-Hall, Englewood Cliffs, New Jersey **1991**, p. 79.
- [5] H. Takeushi, R. J. Roe, *J. Chem. Phys* **1991**, 94, 7446.
- [6] P. Choi, H. P. Blom, T. A. Kavassalis, A. Rudin, *Macromolecules*, **1995**, 28, 8247.
- [7] X. Zhang, Z. Li, Z. Lu, C. Sun, *Macromolecules*, **2002**, 35, 106.
- [8] B. F. Abusharkh, I. A. Hussein, **2002**, *Polymer*, **2002**, 43, 6333.
- [9] H. Sun, S. J. Mumby, J. R. Maple, A. T. Hagler, *J. Amer. Chem. Soc.* **1994**, 116, 2978.
- [10] H. Sun, *J. Comp. Chem.* **1994**, 15, 752.
- [11] H. G. Zachmann, W. L. F. Götz, *J. of Polym. Sci., Polym. Symposia*, **1973**, 42, 693.
- [12] T. Bremner, S. Haridoss, A. Rudin, A. *Polym. Eng. Sci.* **1992**, 32, 939.